2-1996

Variable-Complexity Trellis Decoding of Binary Convolutional Codes

David W. Matolak
University of South Carolina - Columbia, matolak@cec.sc.edu

S. G. Wilson

Publication Info

Postprint version. Published in *IEEE Transactions on Communications*, Volume 44, Issue 2, 1996, pages 121-126.

Matolak, D., Wilson, S. (1996). Variable-Complexity Trellis Decoding of Binary Convolutional Codes. *IEEE Transactions on Communications, 44(2)*, 121-126.
http://dx.doi.org/10.1109/26.486598

Transactions Letters

Variable-Complexity Trellis Decoding of Binary Convolutional Codes

David W. Matolak and Stephen G. Wilson

Abstract—**We consider trellis decoding of convolutional codes with selectable effort, as measured by decoder complexity. Decoding is described for single parent codes with a variety of complexities, with performance "near" that of the optimal fixed receiver complexity coding system. Effective free distance is examined. Criteria are proposed for ranking parent codes, and some codes found to be best according to the criteria are tabulated. Several codes with effective free distance better than the best code of comparable complexity were found. Asymptotic (high SNR) performance analysis and error propagation are discussed. Simulation results are also provided.**

I. INTRODUCTION

REDUCED complexity decoding techniques have attracted much attention in recent years. For code trellises with large numbers of states, reduced-state sequence estimation (RSSE) has been studied as a means of performing near-ML detection with significantly smaller complexity than the conventional Viterbi algorithm (VA). This has been particularly successful in the ISI channel [1]–[3].

Previously, most trellis-coded communication schemes were designed to optimize performance at some fixed receiver complexity, typically on an AWGN channel. Usually free distance is the optimization criterion, supplemented with weight spectrum information. In the scheme proposed here, a single (universal) convolutional encoder is employed at the transmitter, but various receiver decoding complexities are possible. This may be attractive in allowing a family of decoders, with cost proportional to complexity, or possibly in allowing a single processor to be time-shared with other processing tasks from time to time to optimize use of processor resources and/or decoding delay. The trade-off, as usual, is between performance and complexity. We refer to this setting as variable complexity trellis decoding (VCTD).

Anderson and Offer [4] have recently considered the use of RSSE for binary convolutional codes and found that RSSE on (good) codes does not produce better schemes (in terms of free distance) than are obtainable with best codes at a given complexity. Using a more detailed definition of decoder complexity, which takes into account trellis connectivity, we have found several codes which are better in terms of effective free distance than the best known codes of the same complexity. Also, our search has uncovered parent codes that can be decoded with a range of decoder complexities, all the while offering "good" performance, relative to the comparable best code at that complexity.

Here, we measure decoder complexity C as the number of branch metrics computed per decoded bit. Specifically, a (binary) encoder which takes in k bits per unit time has a trellis which has 2^k branches entering or leaving each state, and its decoder must output k information bits per unit time. So, $C = S(2^k/k)$. For encoders with equal values of k, S is a sufficient measure of complexity. For encoders of equal S, however, C increases with k beyond $2S$ when $k > 2$. The encoders studied here have $k = 1$.

The method of RSSE we consider is that in [2]: groups of states in the full trellis are treated as a single subset state, or reduced-trellis (RT) state. These subsets contain $2^p, p = 1, 2, \cdots$, full trellis states. Thus, $\tilde{S} = S/2^p$ states exist in the RT. Decoding is accomplished via a modified Viterbi algorithm, wherein one survivor per subset state is retained at each time stage.

The remainder of this paper discusses these issues in more detail. Section II reviews the method of RSSE, introduces the relevant notation, and defines reduced trellis parameters. Rate $1/n$ codes are the focus. Section II also describes the ranking method we use for these codes and discusses performance. Section III tabulates the resulting best VCTD convolutional codes found by computer search and contains some simulation results.

II. RSSE: METHOD AND REDUCED TRELLIS CONSIDERATIONS

The method and notation used here are best illustrated by example. Fig. 1 shows a diagram of a rate $1/n = 1/2$, memory $m = 3, S = 2^m = 8$ state encoder, and its trellis. Trellis branches are labeled by $u_k; x_k^{(0)}, x_k^{(1)}$, the single input and its associated $n = 2$ outputs. The outputs at any time instant $k, (x_k^{(0)}, x_k^{(1)})$, are described by the convolution of the sequence $\boldsymbol{u}$ with the encoder generator vectors, $\boldsymbol{g}^{(0)}$ and $\boldsymbol{g}^{(1)}$. For the encoder in Fig. 1, these generators, in octal, right-justified notation are (16, 15). The state of this encoder at time k is denoted $\sigma_k = (u_{k-1}, u_{k-2}, u_{k-3})$, ranging here from zero to seven (decimal equivalent).

For state reduction by a factor of two, to yield $\tilde{S} = S/2 = 4$ states in the reduced trellis, the states are grouped in pairs. This

Paper approved by T. Aulin, the Editor for Coding and Communications Theory of the IEEE Communications Society. Manuscript received November 30, 1993; revised June 1, 1994 and August 15, 1994. This paper was presented in part at the Conference on Information Sciences and Systems, Johns Hopkins University, Baltimore, MD, March 24–26, 1993.

D. W. Matolak was with the Department of Electrical Engineering, University of Virginia, Charlottesville, VA 22903 USA. He is now with Loral Communication Systems, Salt Lake City, UT 84116-2988 USA.

S. G. Wilson is with the Department of Electrical Engineering, University of Virginia, Charlottesville, VA 22903 USA.

Publisher Item Identifier S 0090-6778(96)01607-8.

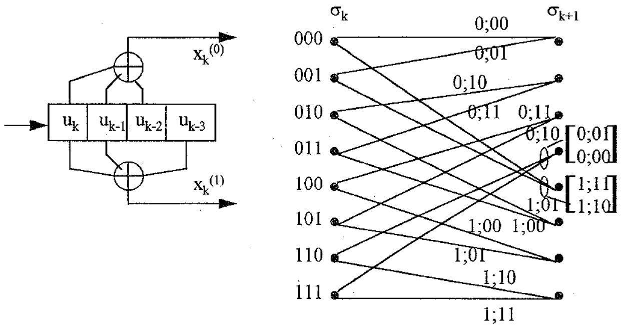

Fig. 1. Rate 1/2, memory $m = 3, S = 8$ state convolutional encoder and its trellis diagram.

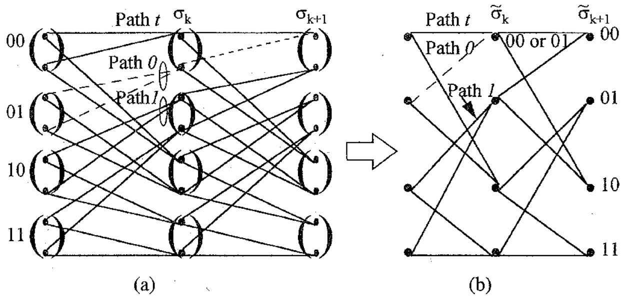

Fig. 2. Illustration of subset grouping on the trellis of Fig. 1 to obtain a reduced trellis of $\tilde{S} = S/2$ states. (a) Grouping in full trellis; (b) equivalent reduced trellis.

grouping is done in a natural way: state 0 is grouped with state 1; state 2 with state 3, and so on. Thus, only the oldest bit u_{k-3} is removed from the state description. The RT state at time k is then $\tilde{\sigma}_k = (u_{k-1}, u_{k-2})$ (Fig. 2). In this manner, by grouping 2^p consecutive full trellis (FT) states together to form each reduced trellis state, any full trellis of S states may be reduced to one having $\tilde{S} = S/2^p$ states. The reduced trellis state description then consists of the first (most recent) $m' = m - p$ bits in the encoder; the other p bits represent a portion of the path history of each subset state, an estimate of which is needed by the decoder to determine which branch symbols to hypothesize.

To decode in the reduced trellis, the VA uses the p estimated bit(s) of the path history, along with the RT state description (effectively the estimated FT state), to address the branch symbols to be used for the next time stage. For example, at time k in the reduced trellis diagram of Fig. 2, the state $\tilde{\sigma}_k = (0, 0)$ may correspond to either full trellis state (0, 0, 0) or (0, 0, 1), depending on which path survives at time k. If the solid line path (Path t) survives, corresponding to *either* of the solid line paths into full trellis state (0, 0, 0) in the associated full trellis diagram, the estimated full trellis state is (0, 0, 0), and the branch symbols $(x_k^{(0)}, x_k^{(1)}) = (0, 0)$ are hypothesized. Similarly, if the dashed path 0 survives, the branch symbols $(x_k^{(0)}, x_k^{(1)}) = (0, 1)$ are hypothesized. The remaining VA operations (add, compare, select for each state) proceed as usual.

In the reduced trellis, we define $\tilde{d}_{\text{free}}$ as the minimum Hamming distance between paths which diverge from the same *subset* state and remerge subsequently at a *subset* state, given that the correct path history is used to label all branches. Thus,

$$\tilde{d}_{\text{free}} = \min_{\boldsymbol{u}: u_1 \neq 0} [wt(\boldsymbol{x})] \tag{1}$$

as long as branches are labeled correctly. Subsequently we call this the *effective free distance*. This condition that branches be labeled correctly simply means using the RT states and their path histories as the estimates of the FT states and labeling branches according to estimated FT state transitions. For reduction by a factor of 2^p, we denote $\tilde{d}_{\text{free}}$ as $\tilde{d}_{\text{free}}^{(2^p)}$. As in full-trellis decoding, this free distance is used to estimate asymptotic [high signal-to-noise (SNR)] performance. For the case of state reduction by a factor of two ($p = 1$), the following theorem applies.

Theorem: For a binary, rate $1/n$, memory m convolutional encoder, with generator vectors $\{\boldsymbol{g}^{(i)}\}$ and free distance d_{free}, the effective free distance in the reduced trellis of $\tilde{S} = S/2 = 2^{m-1}$ states is given by the following formula:

$$\tilde{d}_{\text{free}}^{(2)} = d_{\text{free}} - wt(g_m^{(0)}, g_m^{(1)}, g_m^{(2)}, \cdots g_m^{(n-1)}). \tag{2}$$

Proof: The Hamming distance between any two paths in the reduced trellis is the full trellis distance, decreased by the Hamming distance between the transitions of the final, merging branches of the corresponding full-trellis paths. This Hamming distance is easily computed by noting that a difference in code bits $(x_k^{(i)})$ for these branches appears only where $g_m^{(i)}$ is a one, since only in this bit do the FT states differ. The loss of Hamming distance, associated with the loss of the final merging transitions of the full-trellis paths, is described by the weight of the vector of $g_m^{(i)}$, which yields (2). □

For state reduction by a factor larger than two $(p > 1)$, $\tilde{d}_{\text{free}}$ can be bounded. For $p = 2, 3, 4, \cdots$, a lower bound is obtained via

$$\tilde{d}_{\text{free}}^{(2^p)} \geq \tilde{d}_{\text{free}}^{(2)} - \max_{u_r \in (0,1)} \left[\sum_{j=1}^{p-1} wt(\tilde{\boldsymbol{x}}_j) \right] \tag{3}$$

where $r = 1, 2, \cdots p - 1$, addition of the weights is conventional integer addition, and $\tilde{\boldsymbol{x}}_j$ is defined as $\tilde{\boldsymbol{x}}_j = (x_j^0, x_j^1, \cdots x_j^{n-1})$ with components computed from

$$x_j^i = g_{m-j}^i \oplus g_{m-j+1}^i u_1 \oplus g_{m-j+2}^i u_2 \oplus \cdots \oplus g_{m-1}^i u_{j-1} \oplus g_m^i u_j$$

and the $\oplus$ denotes modulo-2 addition.

An upper bound on $\tilde{d}_{\text{free}}^{(2^p)}$ can be obtained by a simple modification of Heller's bound, as follows:

$$\tilde{d}_{\text{free}}^{(2^p)} \leq \min_{j \geq 1} \left[\frac{2^{j-1}}{2^j - 1} (m - p + j) n \right]. \tag{4}$$

To rank these encoders, we define the state *contour* vector $\boldsymbol{S} = [S, S/2, S/4, \cdots S/2^p]$, and its associated distance *contour* vector $\boldsymbol{d} = [d_{\text{free}}, \tilde{d}_{\text{free}}^{(2)}, \tilde{d}_{\text{free}}^{(4)}, \cdots \tilde{d}_{\text{free}}^{(2^p)}]$. An overall ranking parameter, $\Delta \boldsymbol{d}$ is then computed by comparing the elements of $\boldsymbol{d}$ to the best d_{free} achieved with full trellis decoding, at the corresponding state size (and complexity)

$$\Delta \boldsymbol{d} = \sum_{p=0}^{p_{\max}} [d_{fO}^{(S/2^p)} - \tilde{d}_{\text{free}}^{(2^p)}] \tag{5}$$

where $\tilde{d}^{(\alpha)}_{\text{free},0}$ is the free distance of the optimal free distance (OFD) code of α states. Thus, $\Delta \boldsymbol{d}$ represents the sum of the losses (or gains) in free distance with respect to the OFD codes achievable at the same complexity, and, we suggest, a simple measure of a code's strength under various decoding complexities. For example, for a state contour $\boldsymbol{S} = [256, 128, 64, 32, 16]$, the corresponding full-trellis distance contour of the optimal rate-1/2 free distance codes is $\boldsymbol{d} = \boldsymbol{d}_{\text{OFD}} = [12, 10, 10, 8, 7]$. (Note that this represents five *different* encoders.) For the *single* encoder with $S = 256$ states and generators (472, 557), we have found $\boldsymbol{d} = [12, 11, 9, 8, 6]$ (see Table I). Thus $\Delta \boldsymbol{d} = 1$. The bound of (3) is achieved for this code, i.e., equality holds in (3) for all the elements of $\boldsymbol{d}$.

The significance of $\tilde{d}_{\text{free}}$ is in predicting high SNR error performance, analogous to full trellis decoding. We first define $P_{fe}(k)$ as the probability that the decoder discards the correct (RT) path for the first time at time k. For any finite depth into the trellis, say time k, the distances to all error paths range from $\tilde{d}_{\text{free}}$ to $\tilde{d}_{\max}(k)$. With a union bound argument, we can bound $P_{fe}(k)$ as follows:

$$P_{fe}(k) \leq \sum_{\tilde{d}=\tilde{d}_{\text{free}}}^{\tilde{d}_{\max}(k)} N_{\tilde{d}} P_2(\tilde{d}) \leq \sum_{\tilde{d}=\tilde{d}_{\text{free}}}^{\infty} N_{\tilde{d}} P_2(\tilde{d}) = \tilde{P}_{fe} \quad (6)$$

where $P_2(\tilde{d})$ is the two-codeword error probability for codewords a distance $\tilde{d}$ apart, $N_{\tilde{d}}$ is the number of paths at distance $\tilde{d}$, and we have defined the second sum as $\tilde{P}_{fe}$. At high signal-to-noise ratios, the sum in (6) is dominated by its first term, a function of $\tilde{d}_{\text{free}}$. So, a good approximation to the first error event probability (at any time k) may be obtained by using only this first term.

An RT error event occurs when the decoder chooses a path which diverges from and then remerges with the correct RT path. A general error event probability can also be defined, without regard to the notion of a "first event" [9]. The probability of an error event at any time $k, P_{\text{ev}}(k)$ is the probability that the decoder selects an incorrect path at time k. Note that if a prior error event has occurred, the decoder is no longer selecting between the overall correct and an incorrect path, but between two incorrect paths. In the FT, this is of little consequence, since the (VA) decoder always selects the maximum likelihood path, and an error event always terminates on the true FT state. But, in RT decoding, the occurrence of an error event may in fact increase the probability of subsequent error events, at least until the true FT state is recovered. This error propagation ultimately affects the bit error probability.

In many cases P_{fe} may be the parameter of interest, for example, in cases where the *frame* or *block* error probability is most important. For a frame of length N stages, we define the frame error probability, $P_F(N)$, as the probability that any error event occurs in the length-N frame. (Note that this probability approaches unity at any finite SNR as N becomes large.) We may overbound this probability by a union bound also, using the quantities in (6)

$$P_F(N) \leq \sum_{k=m'-1}^{N} P_{fe}(k) \leq N \cdot P_{fe}(k) \leq N \cdot \tilde{P}_{fe}. \quad (7)$$

TABLE I

$\boldsymbol{d}$ CONTOURS, $\Delta \boldsymbol{d}$ VALUES, AND GENERATOR VECTORS FOR BEST $R = 1/2, R = 1/3$, AND $R = 1/4$ VCTD CODES. THE GENERATORS WHICH YIELD $\tilde{d}^{(2)}_{\text{free}}$ BETTER THAN ANY KNOWN CODE OF THE SAME COMPLEXITY ARE ASTERISKED. GENERATORS WHICH YIELD OFD (O) OR OPTIMUM-DISTANCE-PROFILE (P) CODES OF S STATES ARE ALSO NOTED

m	d	Δd	$(g^{(0)},g^{(1)})$
3	[6,5,3]	0	(16,13),(16,15)
4	[7,5,4,3]	2	(23,35)O,(27,31),(31,33),(31,35)
5	[8,7,6,4,3]	1	(64,57),(54,75)
	[8,7,7,7,3]	1	(72,57)
	[8,6,6,5,3]	1	(51,75),57,73)
6	[9,8,6,6,5 _]	2	(132,163)
	[10,8,7,5,4, _]	2	$(135,147)^P,(133,171)^O$
7	[10,8,8,7,6, _, _]	2	(255,361),(263,367),(265,361),(277,323),(325,361)
8	[12,11,9,8,6, _, _, _]	1	(472,557)*
	[12,10,9,7,7, _, _, _]	2	$(561,753)^O$
9	[12,11,10,9,8, _, _, _, _]	2	(1154,1725)
10	[14,13,11,10,9, _, _, _, _, _]	1	(3346,2751)*,(3662,2647)*

a) rate 1/2 codes, **S** =[1024,512,256,128,64,32,16,8,4,2], $\mathbf{d}_{\text{HB}}$=[14,13,12,11,10,8,8,6,5,4] $\mathbf{d}_{\text{OFD}}$=[14,12,12,10,10,8,7,6,5,3]

m	d	Δd	$(g^{(0)}, g^{(1)},g^{(2)})$
3	[10,7,5]	1	$(13,15,17)^{O,P}$,(15,15,17)
4	[12,9,7,5]	2	$(25,33,37)^O$
5	[13,10,9,7,5]	4	(51,67,75),(51,73,75),(53,71,75),(57,65,71)
6	[15,12,10,8,8, _]	5	(125,163,167),(127,163,165)
			(127,153,171),(135,151,173), (151,153,175)

b) rate 1/3 codes, **S** =[64,32,16,8,4,2], $\mathbf{d}_{\text{HB}}$=[15,13,12,10,8,6], $\mathbf{d}_{\text{OFD}}$=[15,13,12,10,8,5]

m	d	Δd	$(g^{(0)}, g^{(1)}, g^{(2)},g^{(3)})$
3	[12,10,7]	1	(12,16,15,17),(16,16,13,15)
4	[16,12,10,7]	1	(25,33,35,37)
5	[18,14,12,10,7]	3	(51,65,73,77),(51,67,73,75),$(53,67,71,75)^O$

c) rate 1/4 codes, **S**=[32,16,8,4,2], $\mathbf{d}_{\text{HB}}$=[18,16,13,10,8], $\mathbf{d}_{\text{OFD}}$=[18,16,13,10,7]

This bound may be rather loose, but at high SNR, and for modest values of N, a good approximation to $P_F(N)$ may be obtained by using only the first term in $\tilde{P}_{fe}$, i.e., $P_F(N) \cong N \cdot N_{\tilde{d}_{\text{free}}} \cdot P_2(\tilde{d}_{\text{free}})$.

III. CODE SEARCH RESULTS

Tables I–III present the results of a code search. The table entries are the RT effective free distance contours $\boldsymbol{d}$, figure of merit $\Delta \boldsymbol{d}$, and encoder generator vectors (octal, right justified). Also listed for comparison are the upper bounds on the free distances ($\boldsymbol{d}_{\text{HB}}$—Heller's bound for rate $1/n$ codes and $\boldsymbol{d}_{\text{UB}}$ for the rate k/n codes) and the OFD distance contours $\boldsymbol{d}_{\text{OFD}}$. The search was exhaustive.

It is worth noting that these OFD codes are all the "conventional" type, i.e., the encoder takes in k bits per unit time and outputs n bits, for k and n relatively prime. Codes which have larger k and n but the same rate k/n, have higher connectivity and hence higher complexity. In [10], Lee found several unit-memory codes which meet the upper bound on free distance when the conventional codes do not. These codes all have complexity $C > 2S$, whereas the codes here all have complexity $C = 2S$ (see Section I).

Table I contains results for rate 1/2 codes of memory order m from three to 10, rate 1/3 codes of memory order three to six, and rate 1/4 codes of memory order three to five. The codes were selected first on the basis of minimal $\Delta \boldsymbol{d}$; among codes with the same $\Delta \boldsymbol{d}$, the ones with the largest $\tilde{d}_{\text{free}}$ at the smallest $\tilde{S}$ were judged best. Often these turned out to be the

TABLE II

$\boldsymbol{d}$ CONTOURS, $\Delta\boldsymbol{d}$ VALUES, GENERATOR VECTORS AND PUNCTURING MATRICES FOR BEST $R = 2/3$ VCTD CODES DERIVED FROM $R = 1/2$ ORIGINAL CODES, $\boldsymbol{S} = [256, 128, 64, 32, 16, 8, 4], \boldsymbol{d}_{\text{UB}} = [8, 8, 8, 6, 6, 4, 4]$, $\boldsymbol{d}_{\text{OFD}} = [8, 8, 7, 6, 5, 4, 3]$

m	d	Δd	$(g^{(0)}, g^{(1)})$	P
3	[4,3]	0	(14,13),(14,15)	10 11
			(13,17)	11 10
4	[4,4,3]	1	(26,31),(26,37)	11 10
	[5,3,3]	1	(31,33)	10 11
5	[6,5,4,3]	0	(44,73)	10 11
6	[6,5,5,4,3]	2	(165,131)	11 10
			(131,165)	10 11
7	[8,6,5,4,3,_]	4	(225,373),(251,337)	10 11
8	[8,7,5,5,4,_,_]	5	(666,515),(666,545)	10 11

TABLE III

$\boldsymbol{d}$ CONTOURS, $\Delta\boldsymbol{d}$ VALUES, GENERATOR VECTORS AND PUNCTURING MATRICES FOR BEST $R = 3/4$ VCTD CODES DERIVED FROM $R = 1/2$ ORIGINAL CODES $\boldsymbol{S} = [128, 64, 32, 16, 8], \boldsymbol{d}_{\text{UB}} = [8, 8, 6, 6, 4, 4], \boldsymbol{d}_{\text{OFD}} = [7, 6, 6, 5, 4, 4]$

m	d	Δd	$(g^{(0)}, g^{(1)})$	P
3	[4]	0	(13,17)	101 110
			(15,17)	110 101
4	[4,3]	1	(34,23),(34,31),(36,23),(36,31)	100 111
			(26,25),(32,25),(36,25)	111 100
5	[4,4,3]	2	(46,71),(46,75)	111 100
	[5,3,3]	2	(43,65)	100 111
6	[6,4,4,3]	2	(135,163)	100 111
			(163,135)	111 100
7	[6,5,4,3,3]	4	(214,325),(250,357)	100 111
			(340,233),(374,233)	100 111

codes with the largest d_{free} as well. We kept $p \leq 5$ to keep the computation time reasonable. As an example of reading Table I, for $m = 6$, the rate 1/2 code with generators (132, 163) has an effective free distance contour of $\boldsymbol{d} = [9, 8, 6, 6, 5]$ for a state contour of $S = [64, 32, 16, 8, 4]$; the 64-state and 16-state $\tilde{d}_{\text{free}}$ values are each one less than the OFD values, hence by (5), $\Delta\boldsymbol{d} = 2$. For all rates and many values of memory order, several codes achieve the same $\Delta\boldsymbol{d}$. The main results of note in Table I are that the first rate-1/2, memory eight code listed achieves the bound ($\tilde{d}_{\text{free}} = 11$) for $S/2 = 128$ states whereas the OFD code of $S = 128$ states does not; a similar statement applies to the rate-1/2, memory 10 codes, where $\tilde{d}_{\text{free}} = 13$ for $S/2 = 512$ states. Thus, asymptotically, the first event error probability for these codes should be better than their full trellis counterparts.

Table II contains results for punctured rate 2/3 codes for memory order m from three to eight. These codes were obtained by puncturing rate 1/2 codes of the given memory order. The puncturing matrices are also listed. The vector of upper bounds $\boldsymbol{d}_{\text{UB}}$ [11] and the achieved optimal free distance vector $\boldsymbol{d}_{\text{OFD}}$ [12] pertain to *any* (conventional) rate 2/3 code, not only punctured codes, so the values achieved for $\Delta\boldsymbol{d}$ are not as good as they might be for comparison with only punctured codes. Table III presents similar results for rate 3/4 codes of memory order three to seven. Variable-complexity decoding of the rate 2/3 and 3/4 codes is done in a way analogous to the rate $1/n$ case.

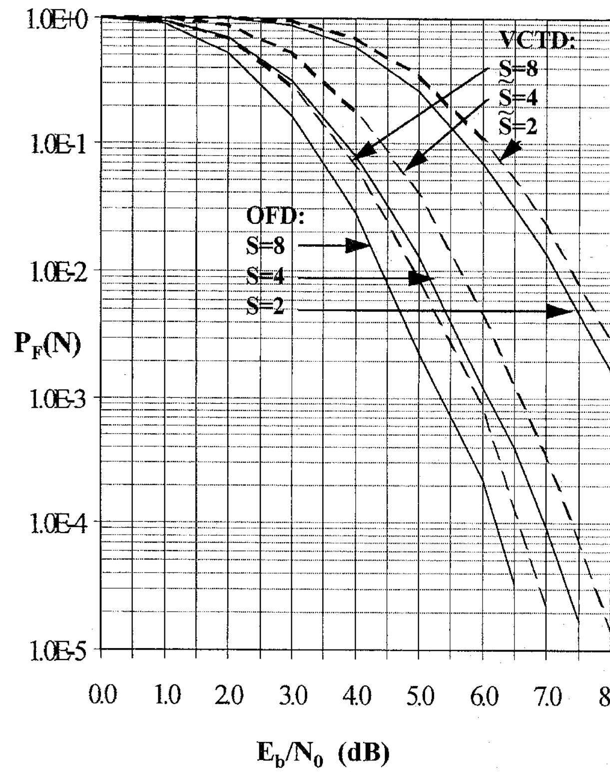

Fig. 3. Frame error probability $P_F(N)$ versus E_b/N_0 for rate 1/2 encoders using binary antipodal signaling on the AWGN channel, and frames of $N = 256$ bits. Solid curves are OFD encoder results of eight, four, and two states, with d_{free} of six, five, and three, respectively; dashed lines are reduced-trellis decoding results for the best $m = 3$ encoder (of Fig. 1) with eight, four, and two states, and $\boldsymbol{d} = [d_{\text{free}}, \tilde{d}^{(2)}_{\text{free}}, \tilde{d}^{(4)}_{\text{free}}] = [6, 5, 3]$.

Unfortunately, none of the best rate 1/2 code generators also appears as original code generators for the other rates. Thus, no *rate-compatible* [13] VCTD codes (rate-compatible across only *two* rates here) have yet been found. Moreover, for no rates other than 1/2 were effective free distances found which exceeded the full trellis OFD values. Nonetheless, these rate-2/3 and rate-3/4 encoders offer the flexibility of VCTD.

To confirm the expected performance, some simulations were conducted. Results for the $S = 8$ state code of Fig. 1 are shown in Fig. 3, which plots $P_F(N)$ versus E_b/N_0 for antipodal signaling on the AWGN channel using frames of $N = 256$ bits. Soft-decision decoding was used, with a 30-bit decoding delay. Two codes with the same effective free distance should have, asymptotically at least, the same frame error probability. In this figure, the solid curves represent the

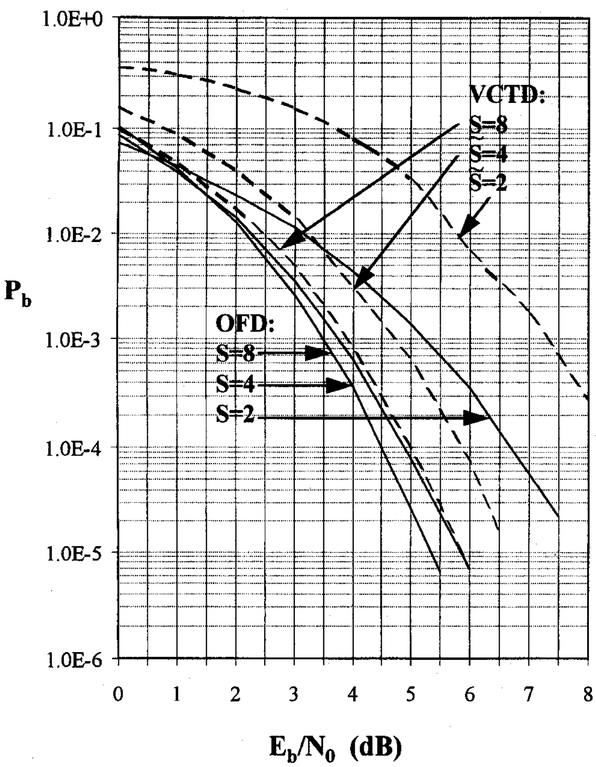

Fig. 4. P_b versus E_b/N_0 for rate 1/2 encoders using binary antipodal signaling on the AWGN channel. Solid curves are OFD encoder results of eight, four, and two states, with d_{free} of six, five, and three, respectively; dashed lines are reduced-trellis decoding results for the best $m = 3$ encoder (of Fig. 1) with eight, four, and two states, and $\boldsymbol{d} = [d_{\text{free}}, \tilde{d}^{(2)}_{\text{free}}, \tilde{d}^{(4)}_{\text{free}}] = [6, 5, 3]$.

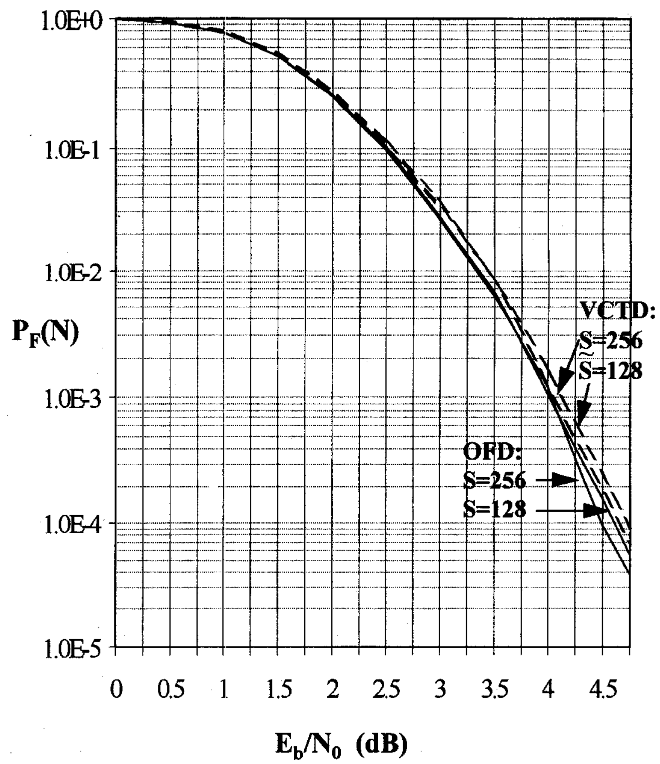

Fig. 5. Frame error probability $P_F(N)$ versus E_b/N_0 for rate 1/2 encoders using binary antipodal signaling on the AWGN channel, and frames of $N = 256$ bits. Solid curves are OFD encoder results of $S = 256$ states ($d_{\text{free}} = 12$), and $S = 128$ states ($d_{\text{free}} = 10$), and the dashed lines are reduced-trellis decoding results for the best $m = 8$ encoder (asterisked in Table I) with $S = 256$ states and $\tilde{S} = 128$ states, with corresponding $\boldsymbol{d} = [d_{\text{free}}, \tilde{d}^{(2)}_{\text{free}}] = [12, 11]$.

decoding performance of the three OFD encoder/decoders of $S = 8, 4,$ and 2 states ($\boldsymbol{d}_{\text{OFD}} = [6, 5, 3]$). The three dashed curves represent the results of VCTD on the encoder of Fig. 1. As noted in Table I, $\boldsymbol{d} = \boldsymbol{d}_{\text{OFD}}$ for this code, so its first event error probability performance should be asymptotically equivalent to that of the OFD codes; the differences in frame error probability at $P_F(N) \approx 10^{-4} - 10^{-5}$ are in good agreement with what is expected due to the increased multipliers ($N_{\tilde{d}}$) of the VCTD trellises. (For $\boldsymbol{S} = [8, 4, 2]$, these VCTD $N_{\tilde{d}}$'s are [5, 5, 2], respectively. The corresponding multipliers for the OFD codes are all one.) In addition, as mentioned following (7), using the dominant term of $\tilde{P}_{fe}$ should yield a good approximation to the frame error probability $P_F(N = 256)$. This holds true for this case, and Table IV compares the approximation and simulation results for the highest-SNR points of each curve on Fig. 3. The *bit* error probability performance, shown in Fig. 4, is also as expected at high SNR. The effect of error propagation appears at low E_b/N_0 (say <7 dB) in Fig. 4, where for $\tilde{S} = 2$, the VCTD code's performance is more than 2 dB worse than that of the OFD code for a given P_b. We also observed no change in performance when the decoding delay was reduced proportionally to the effective encoder memory m', supporting the idea of a variable decoding delay, along with variable complexity.

Simulations were also performed on the rate 1/2, $m = 8$ best VCTD code mentioned previously. As noted in Table I the generators are (472, 557), with an effective free distance of $\tilde{d}^{(2)}_{\text{free}} = 11$ for $\tilde{S} = S/2 = 128$ states, better by one than the OFD code of the same complexity. Fig. 5 plots the frame error probability for this code, decoded with $S = 256$ and $\tilde{S} = 128$ states (dashed lines), and the corresponding results obtained with the two OFD codes of the same complexity (solid lines). As can be seen, for these error rates, the improvement suggested by the larger effective free distance is not realized. This is due to the probably larger error multipliers of the VCTD code, and to the fact that the asymptotic regime is not yet attained at these SNR's. In addition, the performance difference between the *full-trellis-decoded* $S = 256$ state and $S = 128$ state codes is *not* nearly its asymptotic value of 0.8 dB ($10 \log(12/10)$), illustrating the significant effect of the multipliers at these SNR's. Similar results obtain for P_b,

TABLE IV
COMPARISON OF FRAME ERROR PROBABILITY APPROXIMATION $\hat{P}_F(N)$ AND SIMULATED FRAME ERROR PROBABILITY FOR THE CODES OF FIG. 3, WITH $N = 256$

Code	E_b/N_0 (dB)	$\hat{P}_F(N) = N \cdot N_{\tilde{d}_{free}} \cdot P_2(\tilde{d}_{free})$	Simulated $P_F(N)$
OFD, S=8	6.5	5.0×10^{-5}	3.3×10^{-5}
VCTD, S=8	7.0	2.5×10^{-5}	2.2×10^{-5}
OFD, S=4	7.5	1.5×10^{-5}	1.7×10^{-5}
VCTD, $\tilde{S}$ = 4	8.0	1.3×10^{-5}	1.4×10^{-5}
OFD, S=2	8.0	1.8×10^{-3}	1.7×10^{-3}
VCTD, $\tilde{S}$ = 2	8.0	3.6×10^{-3}	2.8×10^{-3}

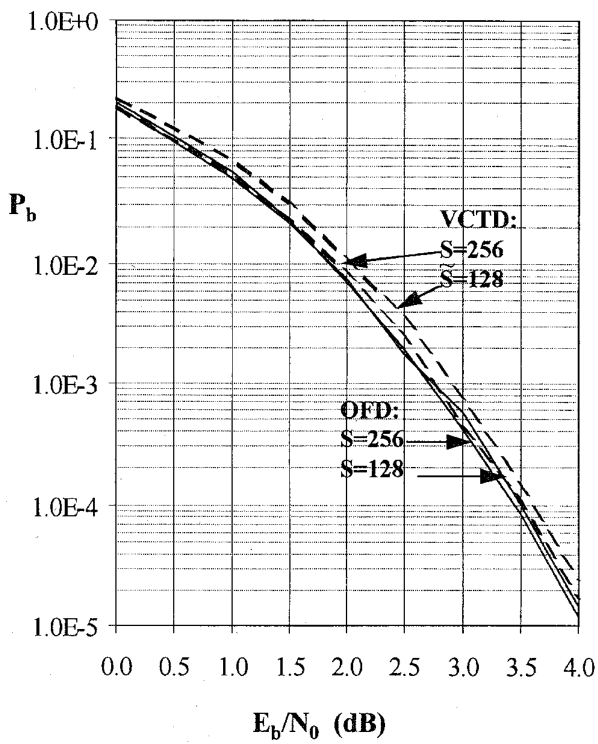

Fig. 6. P_b versus E_b/N_0 for rate 1/2 encoders using binary antipodal signaling on the AWGN channel. Solid curves are OFD encoder results of $S = 256$ states ($d_{\text{free}} = 12$), & $S = 128$ states ($d_{\text{free}} = 10$), and the dashed lines are reduced-trellis decoding results for the best $m = 8$ encoder (asterisked in Table I) with $S = 256$ states and $\tilde{S} = 128$ states, with corresponding $\boldsymbol{d} = [d_{\text{free}}, \tilde{d}^{(2)}_{\text{free}}] = [12, 11]$.

shown in Fig. 6. At higher SNR's though, the first error event probability of the VCTD code should be slightly better than its full-trellis counterpart.

IV. Conclusions

A method of variable-complexity trellis decoding of binary convolutional codes has been described, allowing a single convolutional code to be decoded with various receiver decoder complexities, yielding good performance at each level of complexity. We examined effective free distance, the parameter which predicts asymptotic first error event probability, and obtained bounds on this distance for rate $1/n$ codes. A ranking method was devised for code comparison, and the best VCTD codes of rate $1/n, n = 2$, 3, 4 for short memory order were tabulated. Rate-1/2 codes which have effective free distances better than the best codes of the same complexity were found. Extension of the VCTD idea to codes of rate 2/3 and 3/4 was made by puncturing rate 1/2 codes. The bit error probability of these VCTD codes is degraded by error propagation at low SNR. Asymptotically though, their performance can be as good as, or possibly better, than that of their full-trellis-decoded counterparts, especially in frame error probability.

References

[1] M. V. Eyuboglu and S. U. H. Qureshi, "Reduced-state sequence estimation with set partitioning and decision feedback," *IEEE Trans. Commun.*, vol. COM-36, no. 1, pp. 13–20, Jan. 1988.

[2] A. Duel-Hallen and C. Heegard, "Delayed decision-feedback sequence estimation," *IEEE Trans. Commun.*, vol. 37, no. 5, pp. 428–436, May 1989.

[3] P. R. Chevillat and E. Eleftheriou, "Decoding of trellis-encoded signals in the presence of intersymbol interference and noise," *IEEE Trans. Commun.*, vol. 37, no. 7, pp. 669–676, July 1989.

[4] J. B. Anderson and E. Offer, "Reduced-state sequence detection with convolutional codes," Rensselaer Polytechnic Institute, Tech. Rep. TR-92-5, July 1992.

[5] F. L. Vermeulen, and M. E. Hellman, "Reduced-state Viterbi decoders for channels with intersymbol interference," in *IEEE ICC*, Conference Record, Minneapolis, MN, June 1974, pp. 37B-1 to 37B-4.

[6] F. Jelinek and J. B. Anderson, "Instrumentable tree encoding of information sources," *IEEE Trans. Inform. Theory*, vol. IT-17, pp. 118–119, June 1971.

[7] T. Hashimoto, "A list-type reduced-constraint generalization of the Viterbi algorithm," *IEEE Trans. Inform. Theory*, vol. IT-33, no. 6, pp. 866–876, Nov. 1987.

[8] T. Aulin, "Breadth first maximum likelihood sequence detection," *IEEE Trans. Inform. Theory*, submitted for publication.

[9] S. Lin and D. J. Costello, Jr., *Error-Control Coding: Fundamentals and Applications*. Englewood Cliffs, NJ: Prentice-Hall, 1983.

[10] L. N. Lee, "Short unit-memory byte-oriented binary convolutional codes having maximal free distance," *IEEE Trans. Inform. Theory*, pp. 349–352, May 1976.

[11] E. Paaske, "Short binary convolutional codes with maximal free distance for rates 2/3 and 3/4," *IEEE Trans. Inform. Theory*, vol. IT-20, no. 5, pp. 683–689, Sept. 1974.

[12] J. G. Proakis, *Digital Communications*. New York, NY: McGraw-Hill, 1989.

[13] J. Hagenauer, "Rate-compatible punctured convolutional codes (RCPC Codes) and their applications," *IEEE Trans. Commun.*, vol. COM-36, no. 4, pp. 389–400, April 1988.